Plates

in:
Geology of the Taos Region, Brister, Brian; Bauer, Paul W.; Read, Adam S.; Lueth, Virgil W.; [eds.], New Mexico Geological Society 55 th Annual Fall Field Conference Guidebook, 440 p. https://doi.org/10.56577/FFC-55

This page is intentionally left blank to maintain order of facing pages.

PLATE 1: LANDSAT ETM+ IMAGE – SOUTHERN SAN LUIS BASIN

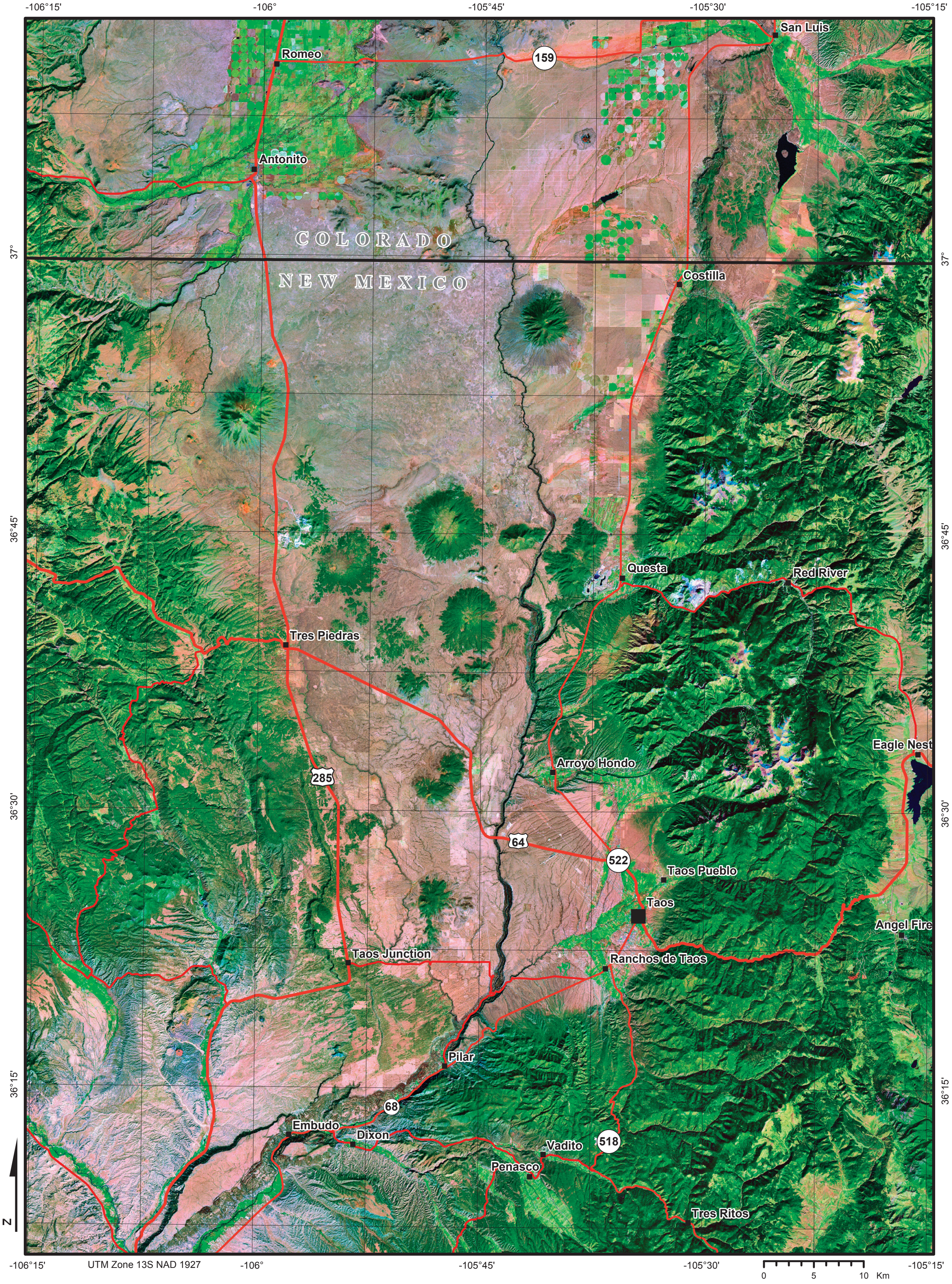

PLATE 1. LANDSAT 7 ETM+ image of the southern San Luis Basin from two scenes acquired 14-Oct-1999. Image processing by Sawyer et al. (2004 – see roadlog references). Bands 7-4-2 (RGB) panchromatically sharpened with 15-meter Band 8 data.

PLATE 2: GENERALIZED GEOLOGIC MAP – SOUTHERN SAN LUIS BASIN

COMPILED BY: ADAM S. READ, REN A. THOMPSON, AND MARK M. MANSELL

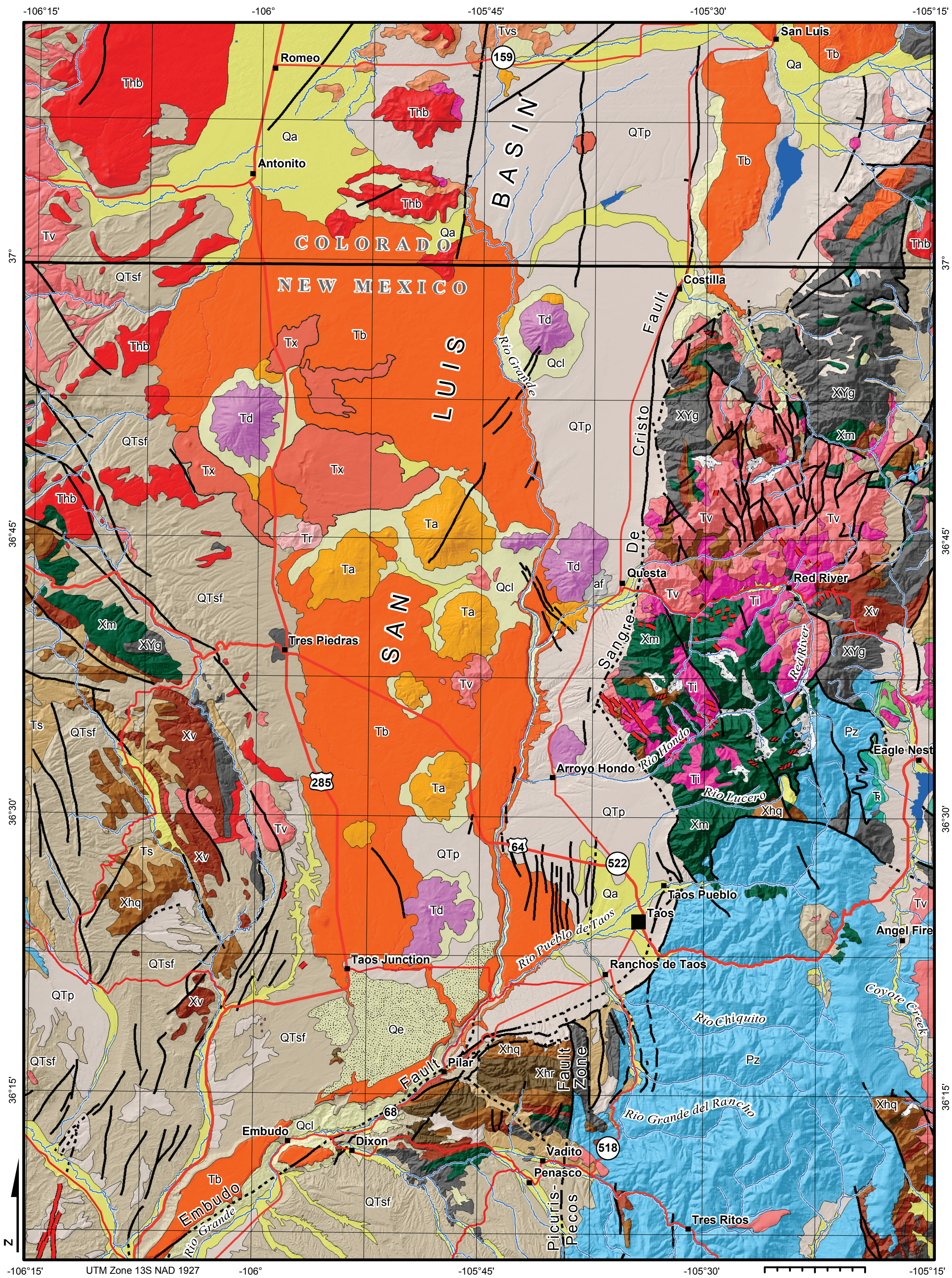

PLATE 2. Geologic map and block diagrams of the southern San Luis Basin area. The geologic map is based largely on 1:500,000 geologic maps of New Mexico and Colorado (NMBGMR, 2004; Tweto, 1979). Taos Plateau volcanic field geology from R.A. Thompson (unpublished mapping) and Taos valley geology from Bauer et al. (Plate 6, this volume). The block diagrams depict the modern configuration of the Proterozoic basement at 2x vertical exaggeration (modified from Plate 2 of Baltz and Myers, 1999).

PLATE 2 – (CONTINUED)

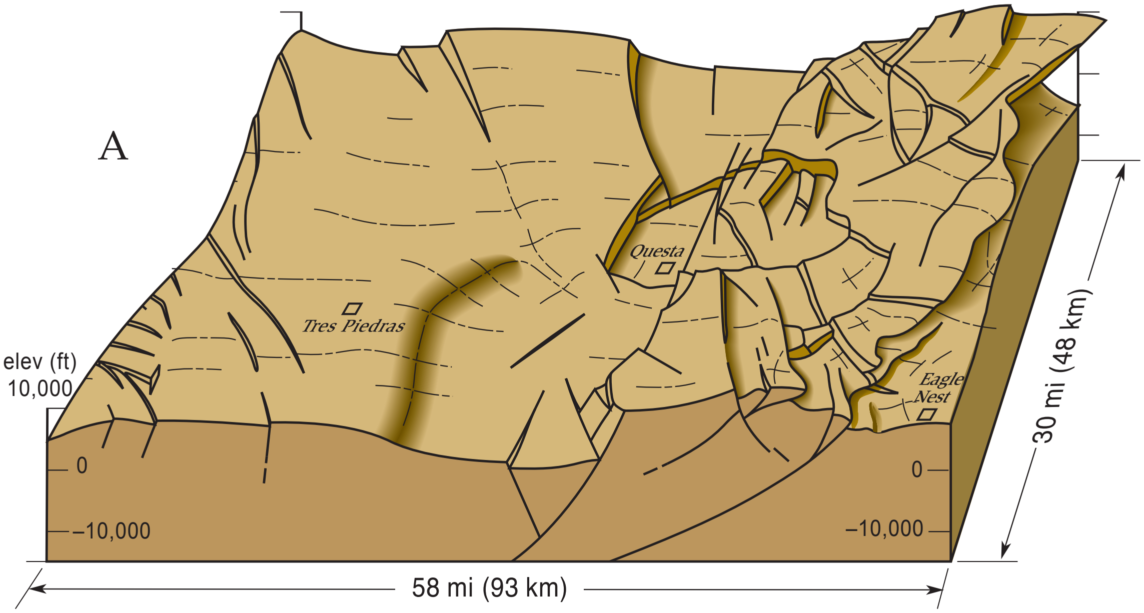

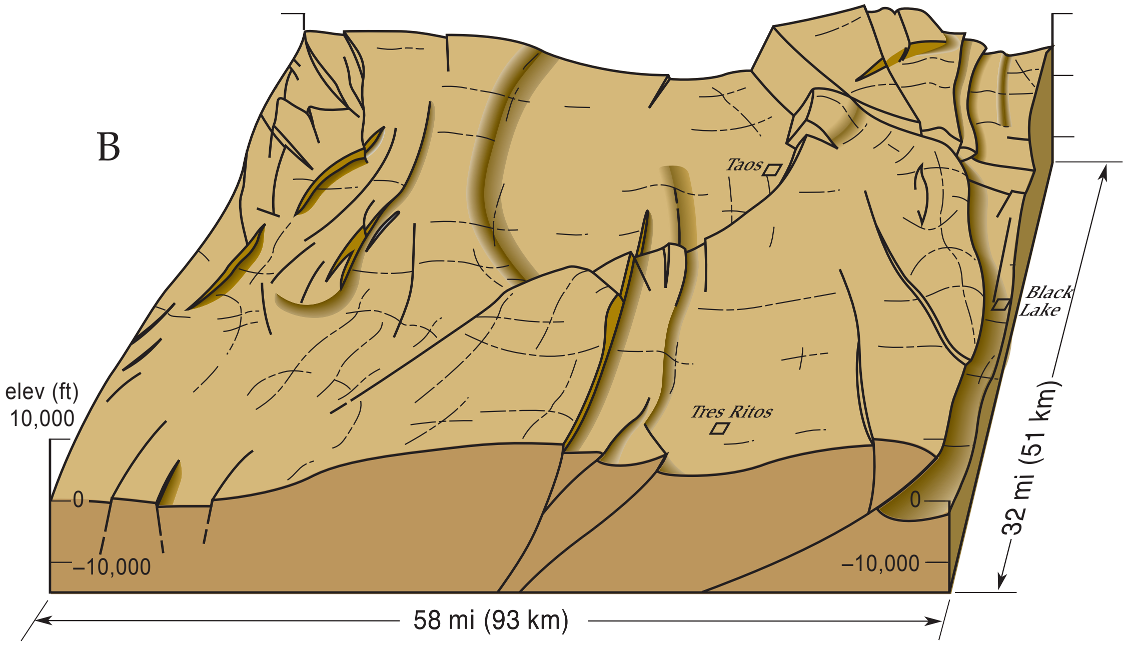

Legend

- fault-approximately located
- fault-exposed
- fault-concealed
- Tertiary dikes
- Neoproterozoic dike

Quaternary

	water
	artificial fill (tailings)
Qa	alluvium
Qe	eolian deposits
Qcl	colluvium and landslides
Qd	glacial deposits (Pleistocene)
QTp	piedmont deposts
QTsf	Santa Fe Group (Miocene to Pleistocene)

Tertiary

Tv	volcanic rocks-undifferentiated
Tx	xenocrystic basaltic andesite (Pliocene)
Td	dacite (Pliocene)
Tb	Servilleta Basalt (Pliocene)
Tr	rhyolite of No Agua Peak (Pliocence)
Ta	olivine andesite (Pliocene)
Thb	Hinsdale Basalt (upper Oligocene to Pliocene)
Ti	intrusive rocks and dikes
Tvs	volcaniclastic rocks and sediments
Ts	sedimentary rocks-undifferentiated

Mesozoic

K	sedimentary rocks-undifferentiated
J	sedimentary rocks-undifferentiated
Ћ	sedimentary rocks-undifferentiated

Paleozoic

Pz	sedimentary rocks-undifferentiated

Proterozoic

XYg	granitic rocks
Xhr	Rinconada Fm. of Hondo Group
Xhq	Ortega Fm. of Hondo Group
Xv	Vadito Group
Xm	mafic plutonic/volcanic rocks

PLATE 3: ISOSTATIC RESIDUAL GRAVITY – SOUTHERN SAN LUIS BASIN

V.J.S. Grauch and G.R. Keller

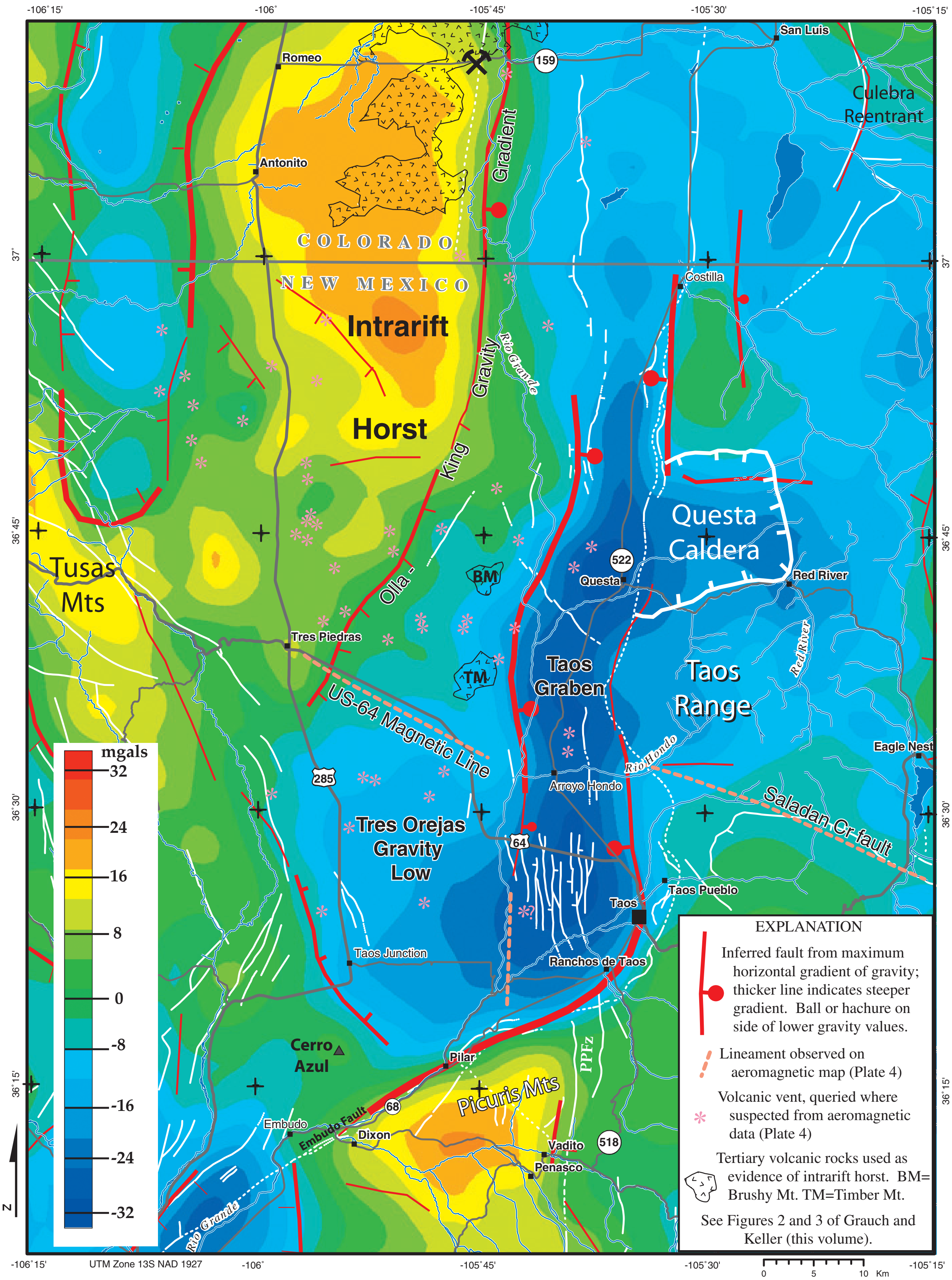

PLATE 3. Color image of isostatic residual gravity data in milligals (mgals) overlain by selected geologic and geophysically interpreted features. Data and interpretations are described in Grauch and Keller (2004 this volume). Mapped faults are shown in white.

PLATE 4: AEROMAGNETIC DATA - SOUTHERN SAN LUIS BASIN

V.J.S Grauch and G.R. Keller

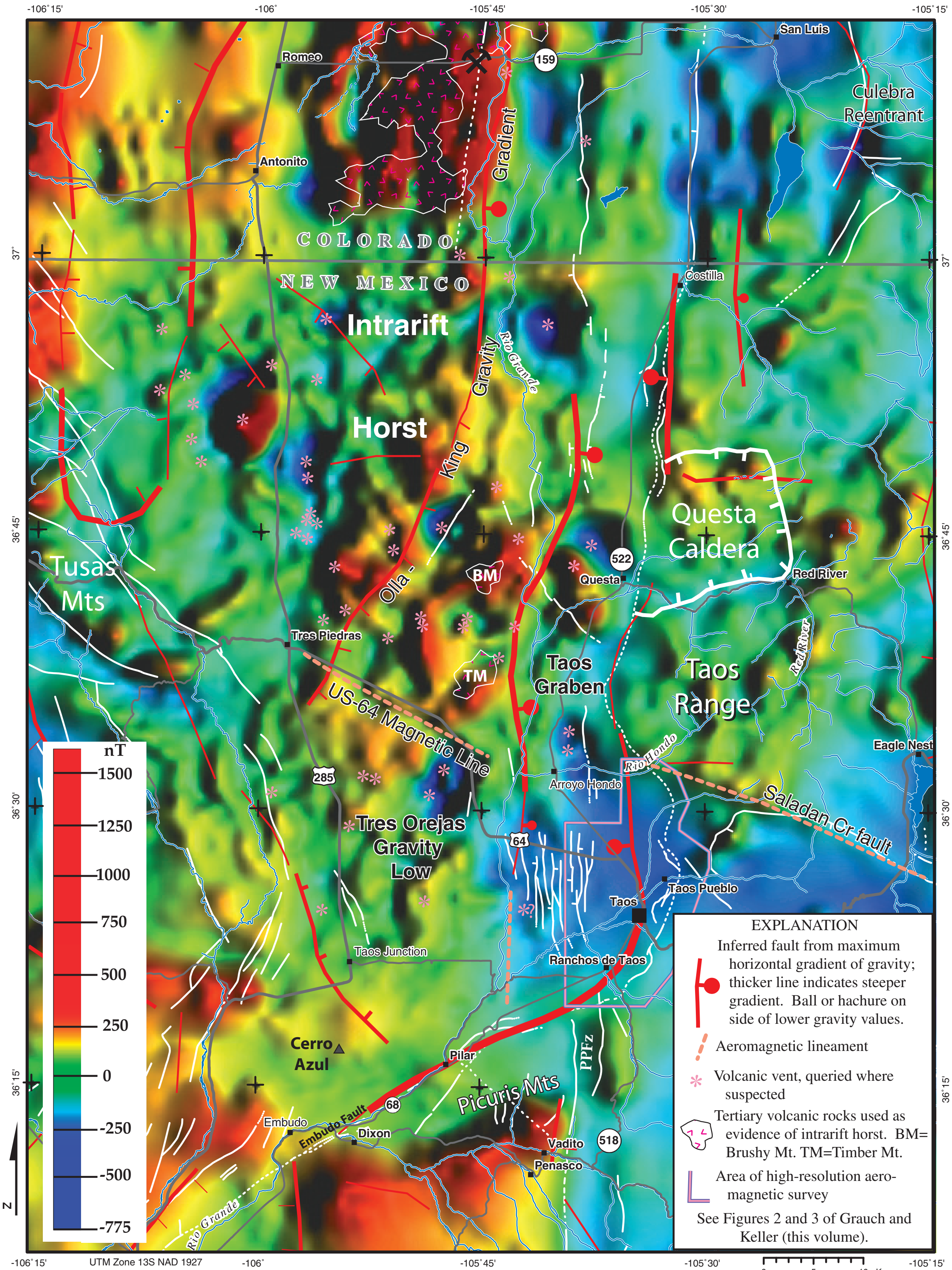

PLATE 4. Color shaded-relief image of reduced-to-pole aeromagnetic data in nanoteslas (nT) overlain by selected geologic and geophysically interpreted features. Data and interpretations are described in Grauch and Keller (2004 this volume). Mapped faults shown in white.

PLATE 5: HIGH-RESOLUTION AEROMAGNETIC DATA – TAOS AREA

V.J.S. Grauch, Paul W. Bauer, and Keith I. Kelson

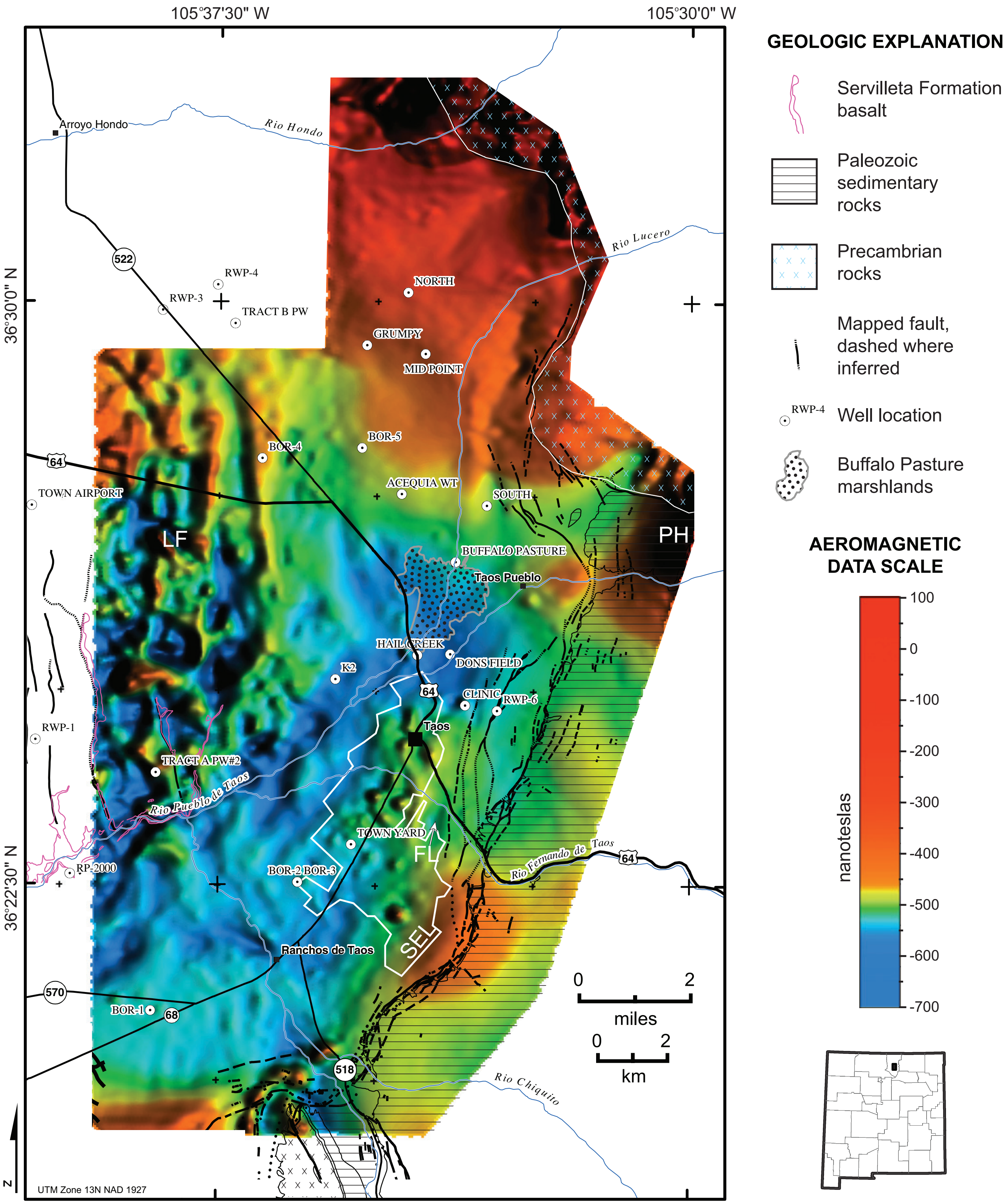

PLATE 5a. Color shaded relief image of reduced-to-pole (RTP), downward-continued, high-resolution aeromagnetic data for the Taos area. White outline indicates the limits of the Town of Taos. LF=landfill. FL=aeromagnetic low near Rio Fernando de Taos. SEL = aeromagnetic high just outside southeast town limits. See Grauch et al. (2004, this volume) for discussion.

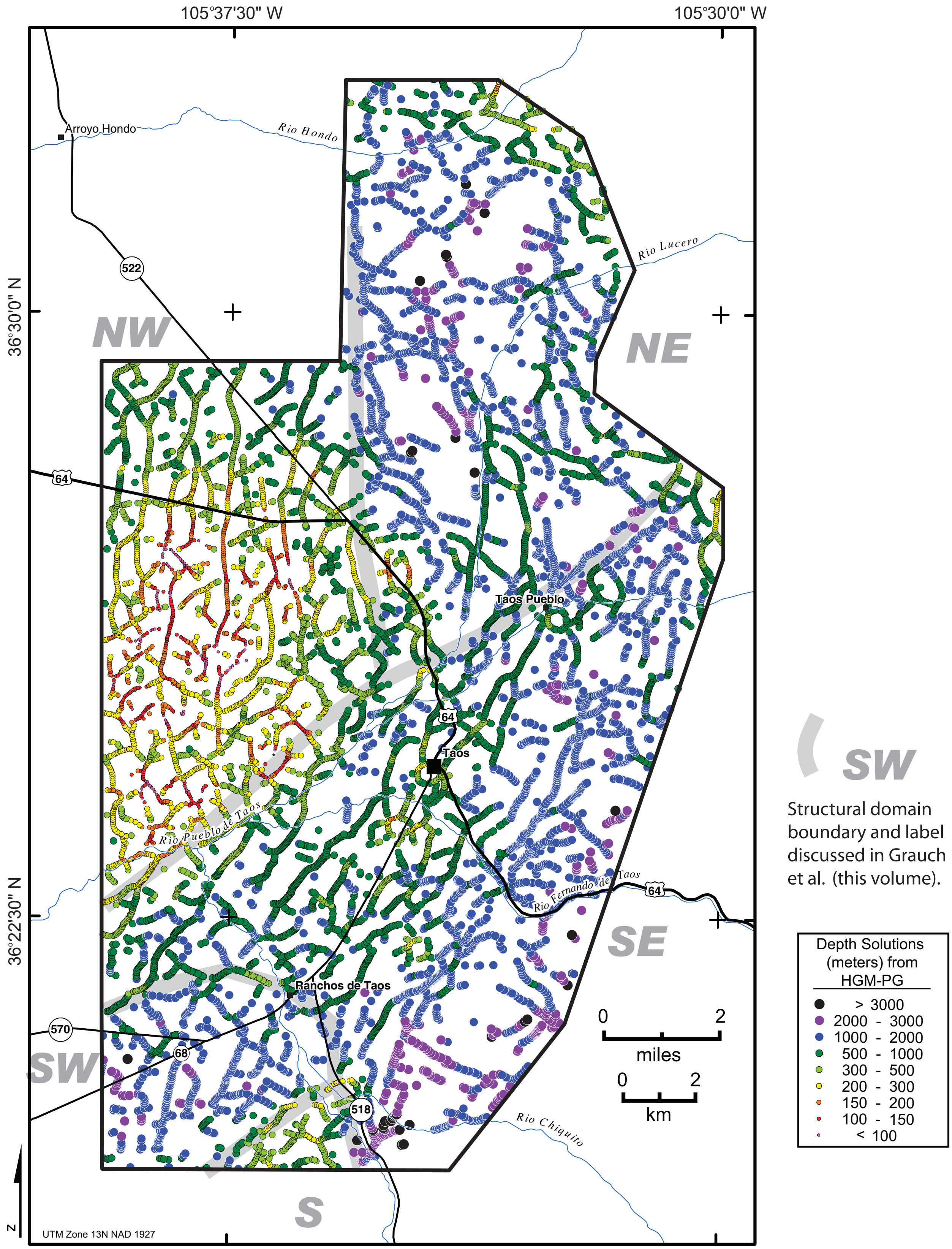

PLATE 5b. Maximum estimates of depth (meters) to the tops of magnetic source edges computed from the horizontal gradient magnitude of pseudogravity (HGM-PG), which is derived from aeromagnetic data (Plate 5a). Each point is an individual solution computed within a moving window across the grid. See Grauch et al. (2004, this volume) for discussion.

PLATE 6: GENERALIZED GEOLOGIC MAP AND CROSS SECTION – TAOS AREA

Paul W. Bauer, Keith I. Kelson, and Adam S. Read

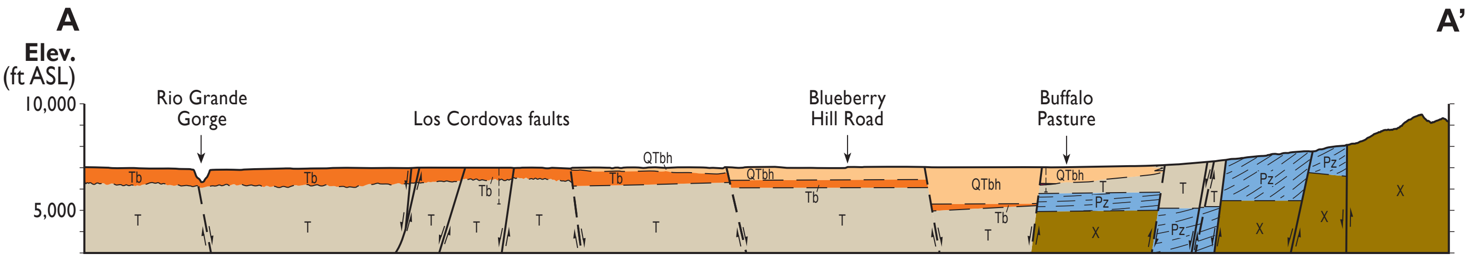

- artificial fill
- breccia
- Qal *alluvium*
- Qm *Buffalo Pasture marsh*
- Qe *eolian deposits*
- Qcls *colluvium and landslide deposits*
- Qt *fluvial terrace deposits*
- Qf *alluvial fan deposits*
- QTbh *Blueberry Hill deposits*
- Tsf *Santa Fe Group basin fill*
- Tb *Servilleta Basalt*
- Tr *rhyodacite cone of Tres Orejas*
- Tp *Picuris Fm.*
- Pz *sedimentary rocks-undifferentiated*
- Xg *granites and granitic gneisses*
- Xhu *upper Hondo Group*
- Xho *Ortega Fm. of Hondo Group*
- Xv *metavolcanic rocks*
- fault-exposed
- fault-approximately located
- fault-concealed
- overturned syncline
- detailed aeromagnetic survey area (see Plate 5)

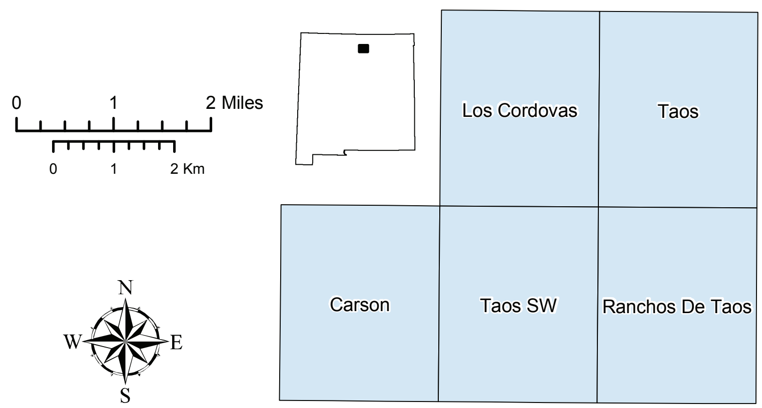

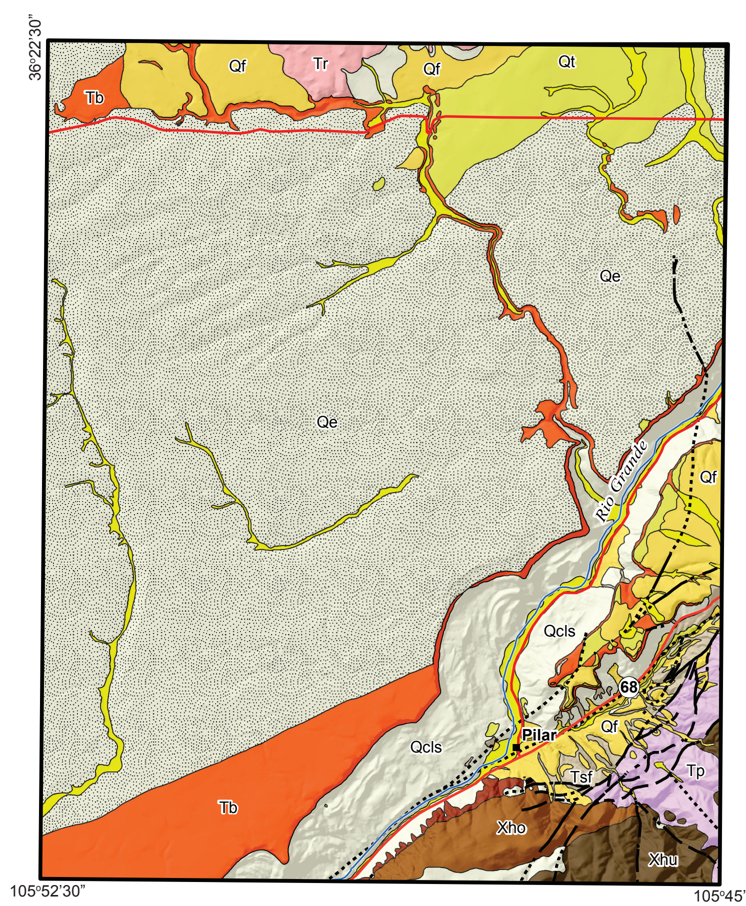

PLATE 6. Geologic map and cross section of the Taos area based on recent 1:24,000 scale mapping by P. Bauer and K. Kelson (see roadlog references for NMBGMR OF-GM series maps of individual quadrangles).

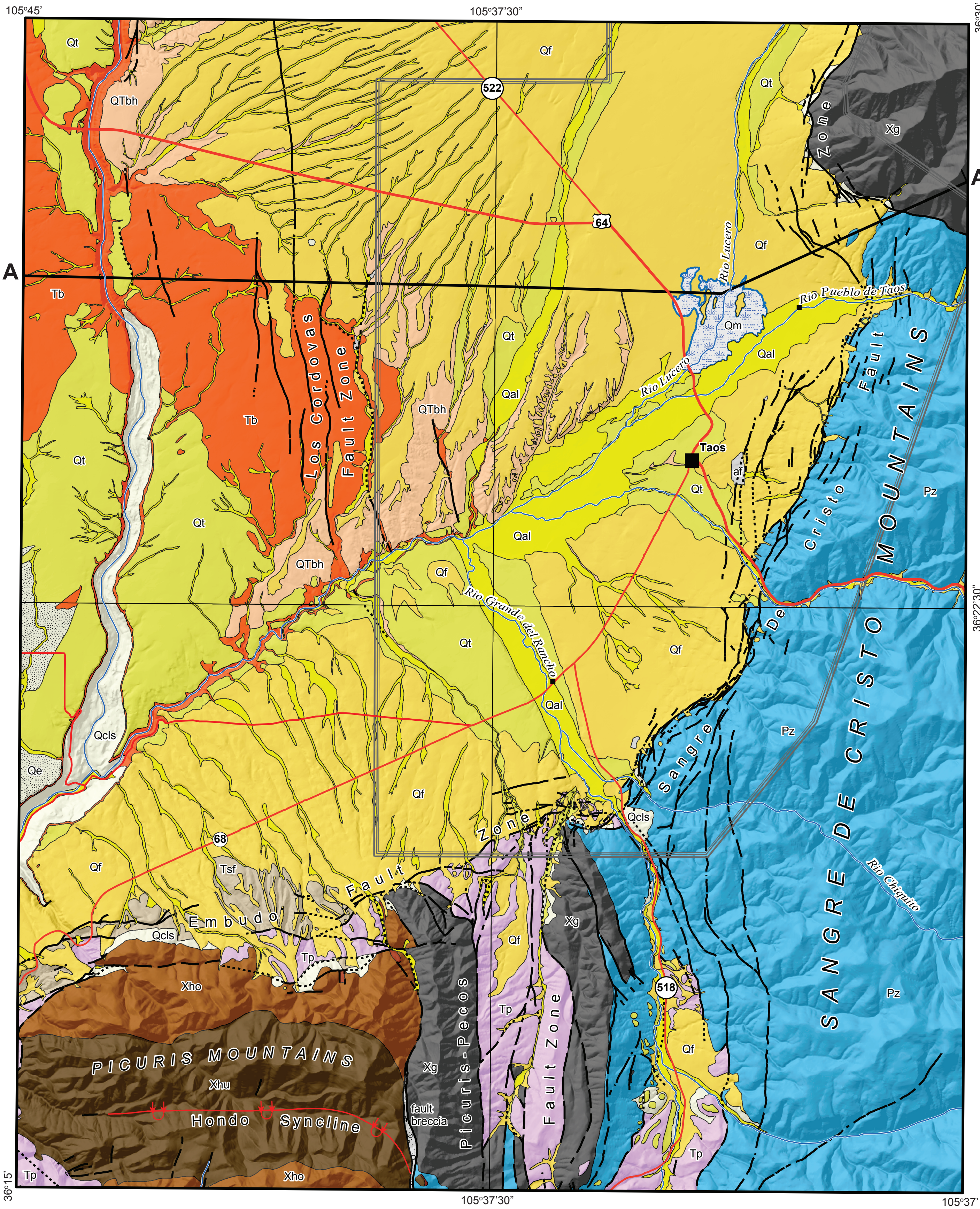
105°45'
105°37'30"
36°30'
A
A'
Qt
QTbh
Qf
522
64
Xg
Zone
Rio Lucero
Qf
Tb
Rio Pueblo de Taos
Qm
Qt
Qal
Los Cordovas
Fault Zone
Tb
QTbh
Qal
Fault
Taos
af
Qt
Qt
Pz
Cristo
MOUNTAINS
Qt
QTbh
Qal
Qf
Rio Grande del Rancho
36°22'30"
Qt
Qf
De
Qal
Qcls
Sangre
Pz
Qe
Qf
Zone
Qcls
68
Qf
Tsf
Fault
Rio Chiquito
Embudo
Qcls
Xg
Tp
Qf
Xho
518
SANGRE DE CRISTO
Tp
Pz
PICURIS MOUNTAINS
Xg
Qf
Xhu
Picuris-Pecos
Fault Zone
Hondo
Syncline
fault breccia
Tp
Tp
Xho
36°15'
105°37'30"
105°37'

PLATE 7: CENOZOIC GEOLOGIC TIMELINE – TAOS AREA

PAUL W. BAUER, KEITH I. KELSON, AND DANIEL J. KONING

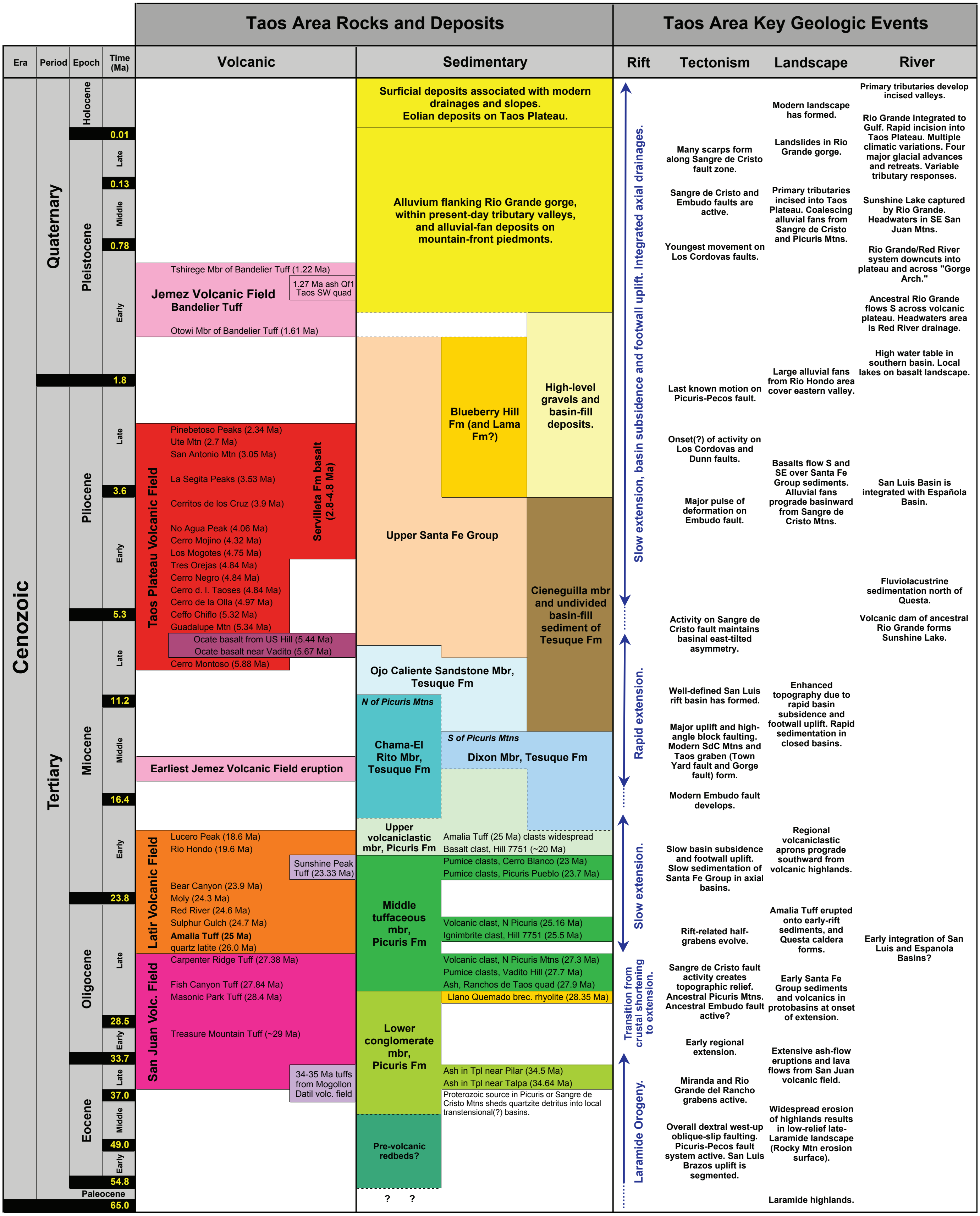

PLATE 7. Timeline of key Cenozoic geologic rocks and events in the Taos area. This chart is designed to display general temporal relationships among the volcanic rocks of the southern San Luis Basin region, the sedimentary units that have been mapped in the Taos area, and a variety of significant geologic events. The data have been synthesized from a great variety of sources, all of which are listed in roadlog references.

PLATE 8: PALEOGEOGRAPHIC MAPS OF THE TAOS AREA

GARY A. SMITH

WITH CONTRIBUTIONS FROM

PAUL W. BAUER AND DANIEL J. KONING

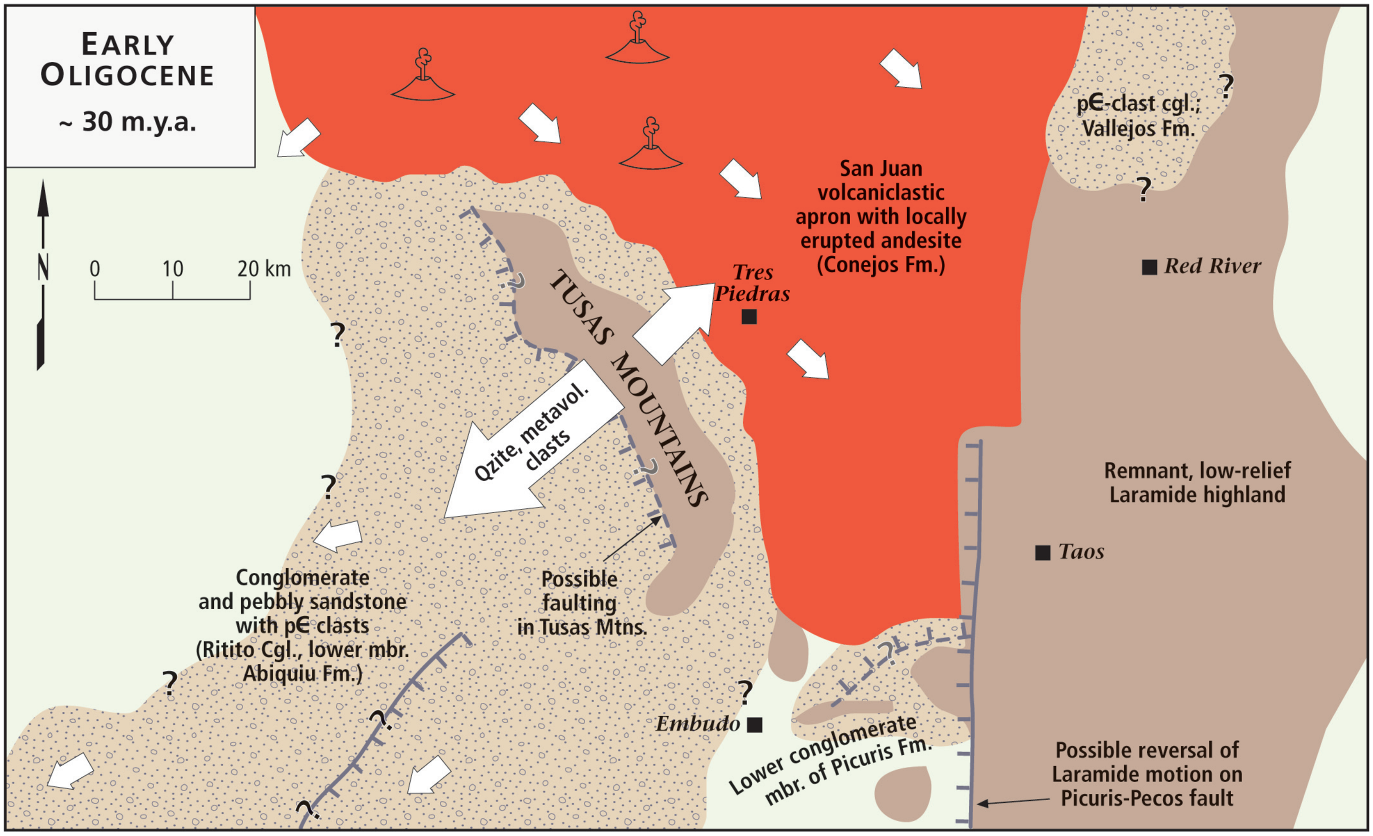

8a) 30 Ma paleogeographic map – Taos area.

PLATE 8 (a-e). Paleogeographic Maps of the southern San Luis Basin from 30 Ma to 5 Ma. This series of maps, modified from Smith (2004; see road log references), schematically illustrate the changing geographic, volcanic, and structural elements of the San Luis Basin and vicinity, in New Mexico, after the Laramide orogeny.

At the close of the Laramide orogeny north-central New Mexico featured a broad uplift largely denuded of Phanerozoic strata. Oligocene structural inversion of Laramide structures outlined the nascent Rio Grande rift, overfilled with volcaniclastic debris. Oligocene volcaniclastic sediments shed southward from the San Juan and Latir volcanic fields intermingle with detritus eroded from Precambrian-rock highlands in the Tusas and Sangre de Cristo Mountains, and Sierra Nacimiento. The Tusas Mountains stood sufficiently high to divert drainages southeastward from the San Juan volcanic field. The Tusas Mountain topographic barrier was overtopped at about the time of eruption of the Amalia Tuff (25 Ma) to form the Questa caldera. Mafic volcanism was widespread in northern New Mexico and southern Colorado.

The middle Miocene geography shows alluvial sediment flooding the rift basins from the north, largely eroded from the extinct San Juan and Latir volcanic fields with locally important contributions from Precambrian-rock uplands. Quartzite detritus from the Truchas Peaks dispersed into the Peñasco area around the northern end of the slowly rising Santa Fe Range. Dixon and Cejita member gravel of admixed Precambrian and Paleozoic clasts marks the course of the ancestral Rio Embudo. Widespread eolianite of the Ojo Caliente Sandstone provides a prominent marker in the regional stratigraphy. Middle Miocene basin-fill sediment and basalt currently preserved at high elevations in the Red River-Valle Vidal area represent part of the eastern step-faulted margin of the San Luis Basin that later rose in the footwall of the Sangre de Cristo fault.

By 10 Ma, strong tilting in the San Luis and Española Basins restricted deposition to areas adjacent to the footwall uplifts. Hypothesized hanging-wall hinge zone rupture that uplifted the Tusas Mountains and Santa Fe Range enhanced basin-floor tilting. The Peñasco embayment formed as a part of the eastern Española Basin not involved in Santa Fe Range uplift, and bounded on the north by the Picuris Range, which uplifted along the Embudo fault. Jemez Mountains volcanic constructional topography deflected drainage eastward to form the Rio Chama as aggradation ceased in most of the Abiquiu embayment at about 10 Ma.

Upper Miocene and Pliocene rocks delineate geography very similar to the present. Deposition in the strongly east-tilted San Luis Basin focused within grabens close to the basin master fault system. Pliocene basalt volcanism formed the Taos Plateau and Ocate volcanic fields. Ocate lava apparently flowed along the course of the ancestral Rio Embudo into the Vadito area, indicating headwaters far to the east of the modern divide. Pliocene deposition in the Moreno and Mora valleys relates to extensional inversion of Laramide thrust faults.

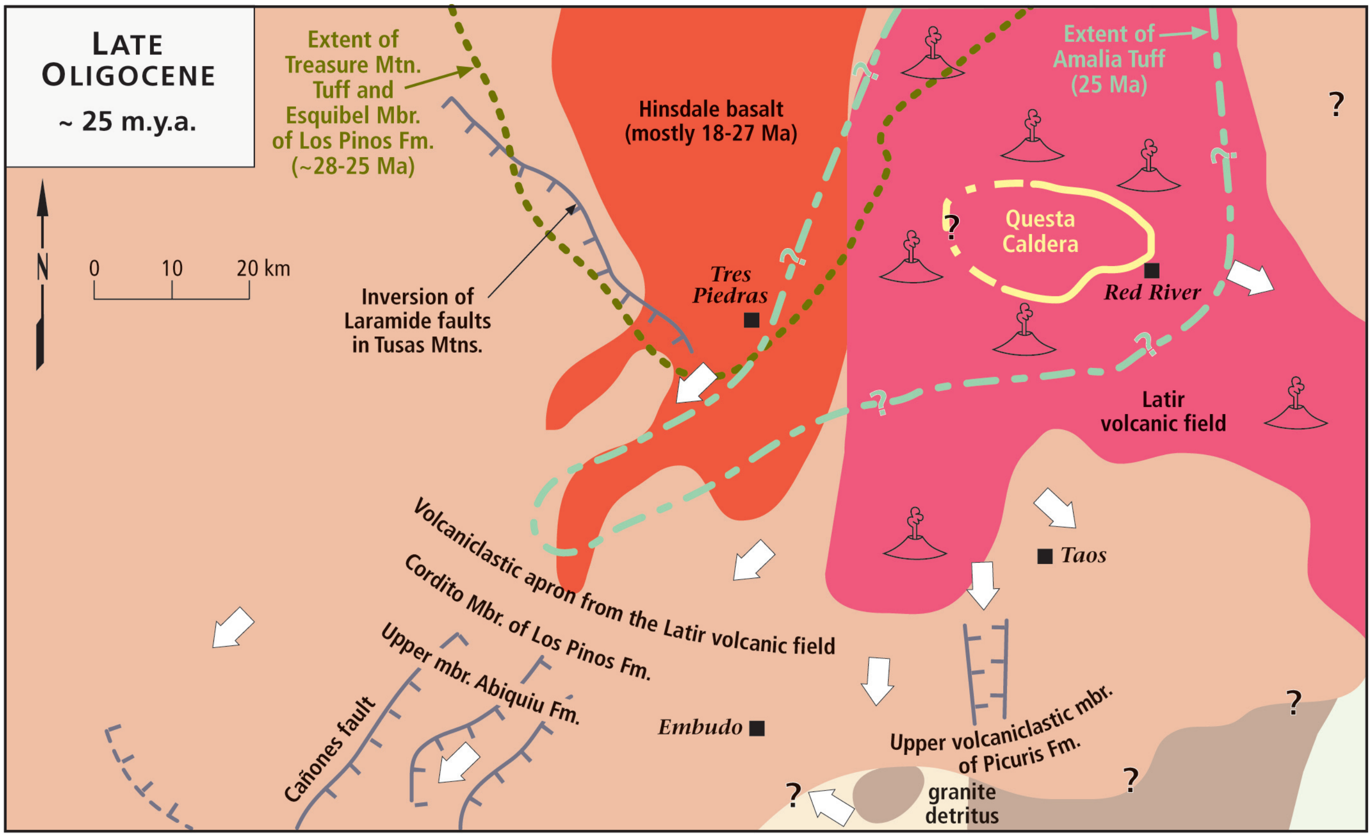

8b) 25 Ma paleogeographic map – Taos area.

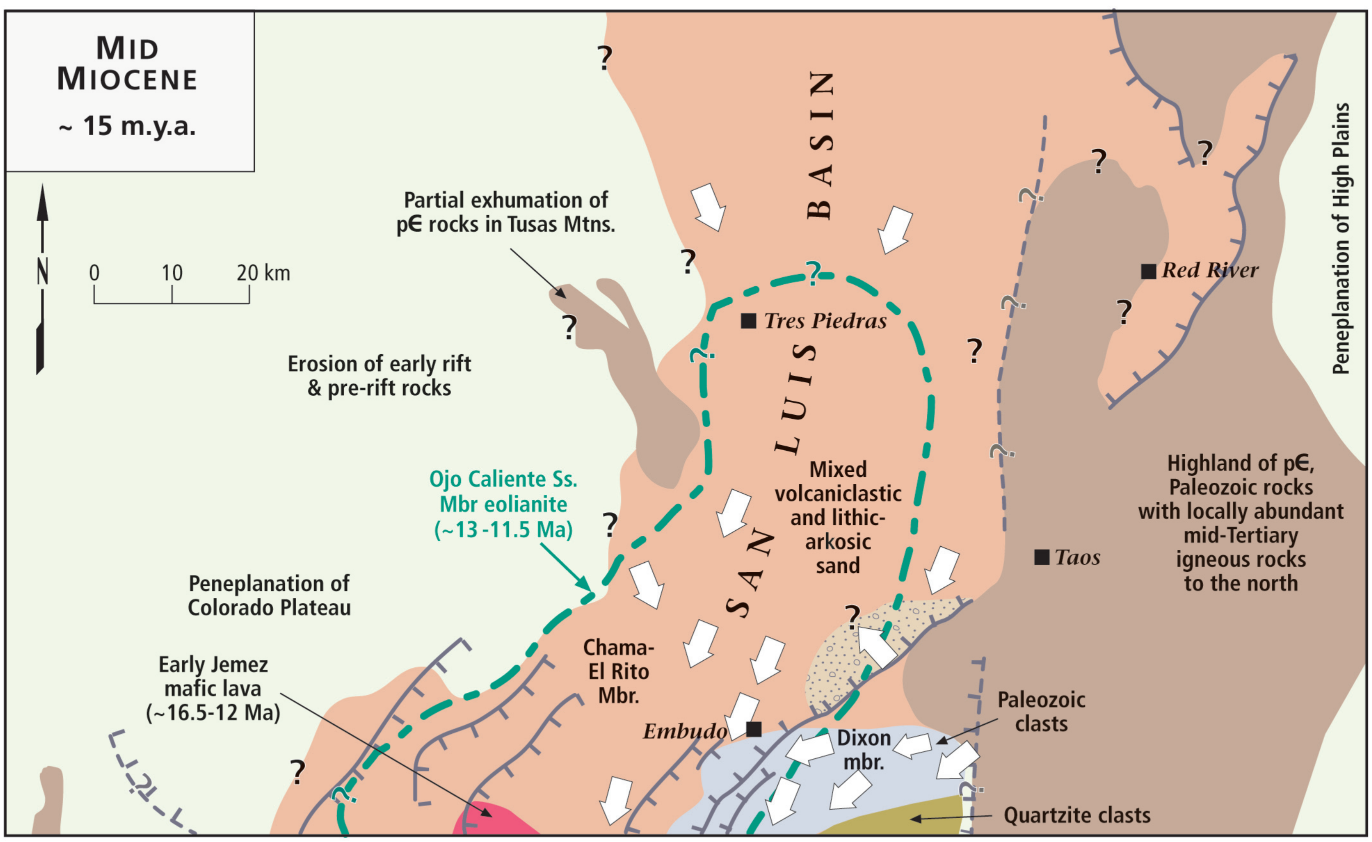

8c) 15 Ma paleogeographic map – Taos area.

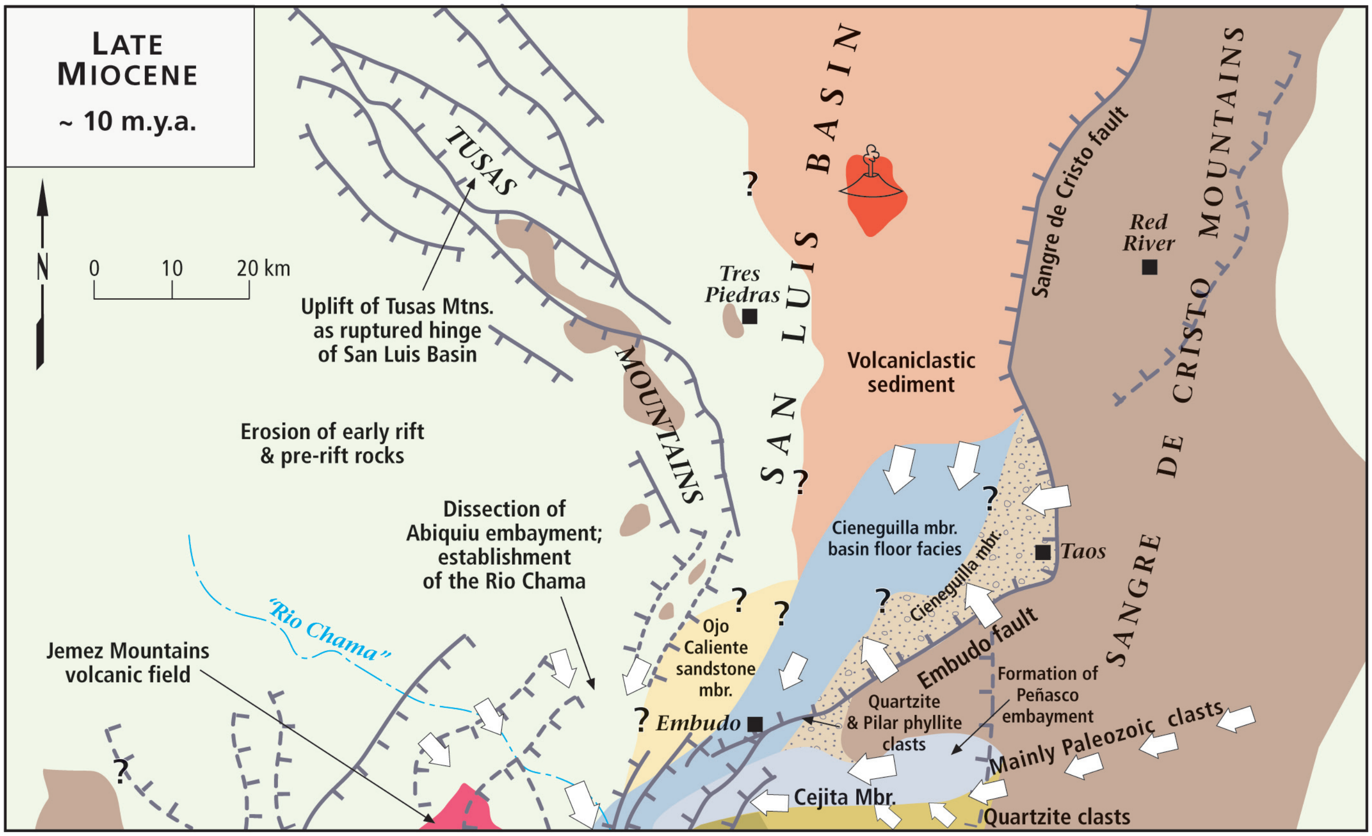

8d) 10 Ma paleogeographic map – Taos area.

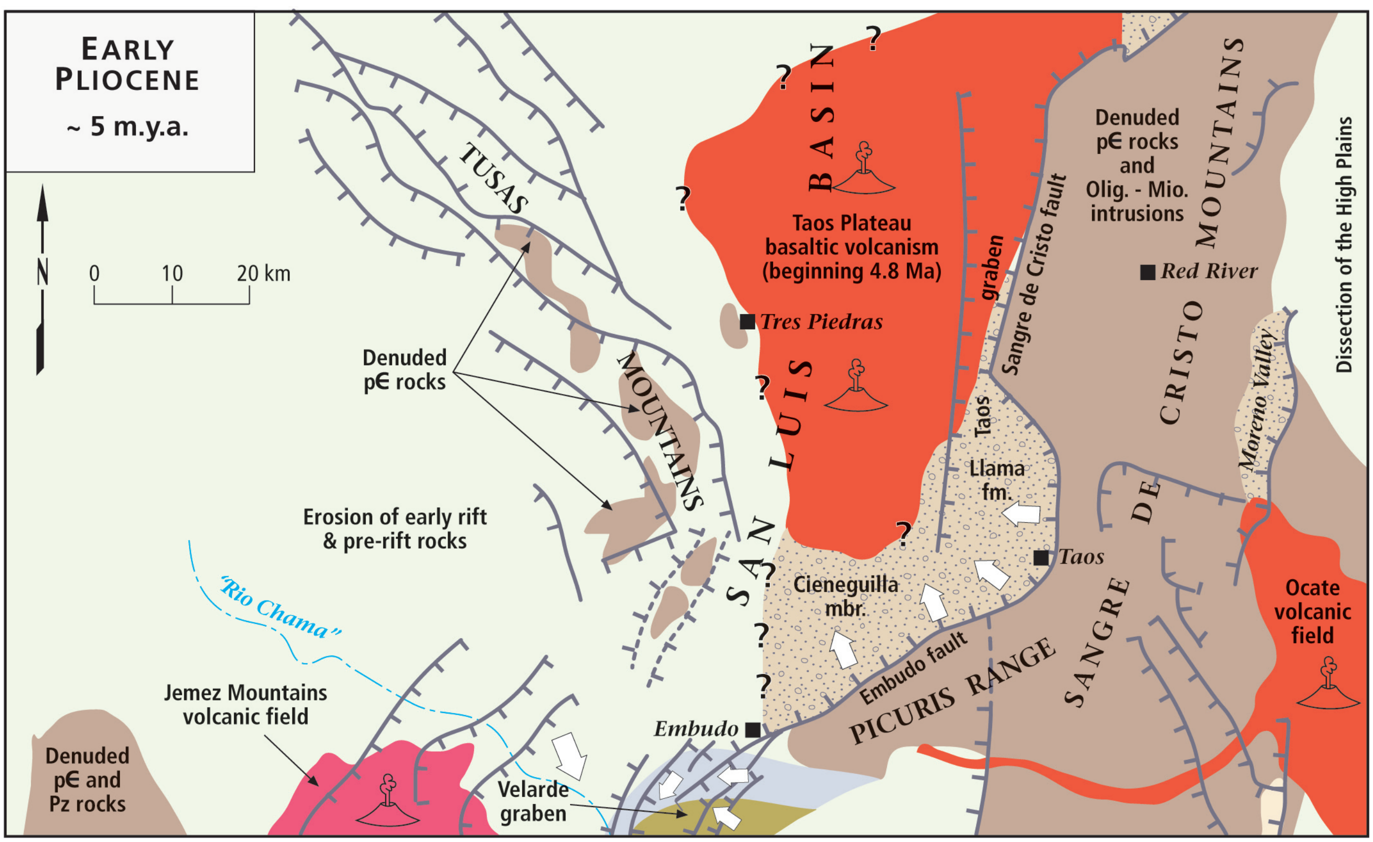

8e) 5 Ma paleogeographic map – Taos area.

PLATE 9: TRENCH PROFILE – SANGRE DE CRISTO FAULT

Keith I. Kelson, Sean D. Connell, Dave W. Love, and Paul W. Bauer

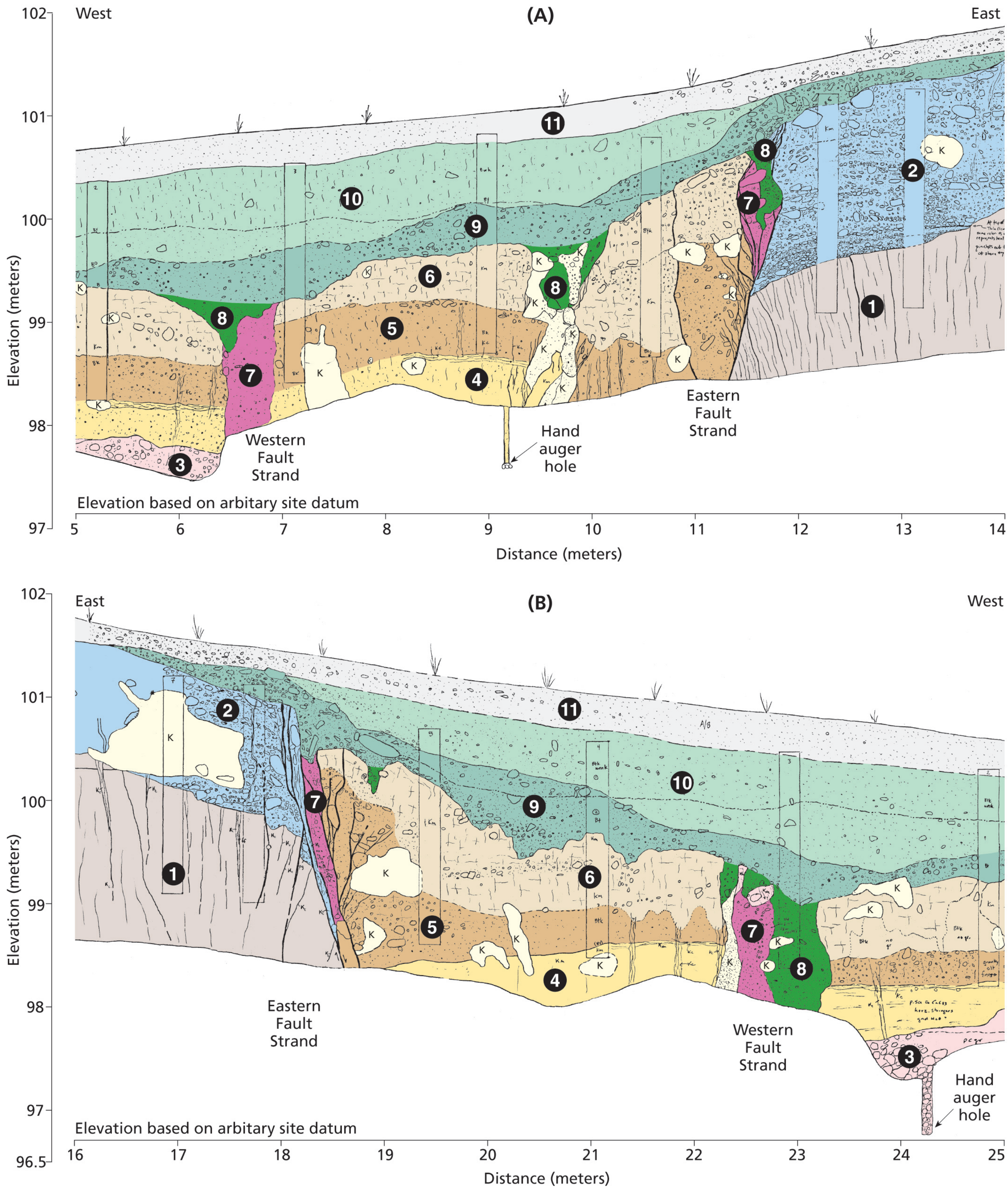

PLATE 9. Detailed trench profiles of the Sangre de Cristo fault exposed in (a) northern wall and (b) southern wall of trench T-1, Taos Pueblo site. For discussion and unit descriptions, see Kelson et al. (2004, this volume) and Appendix A therein. K = krotovina (bioturbation).

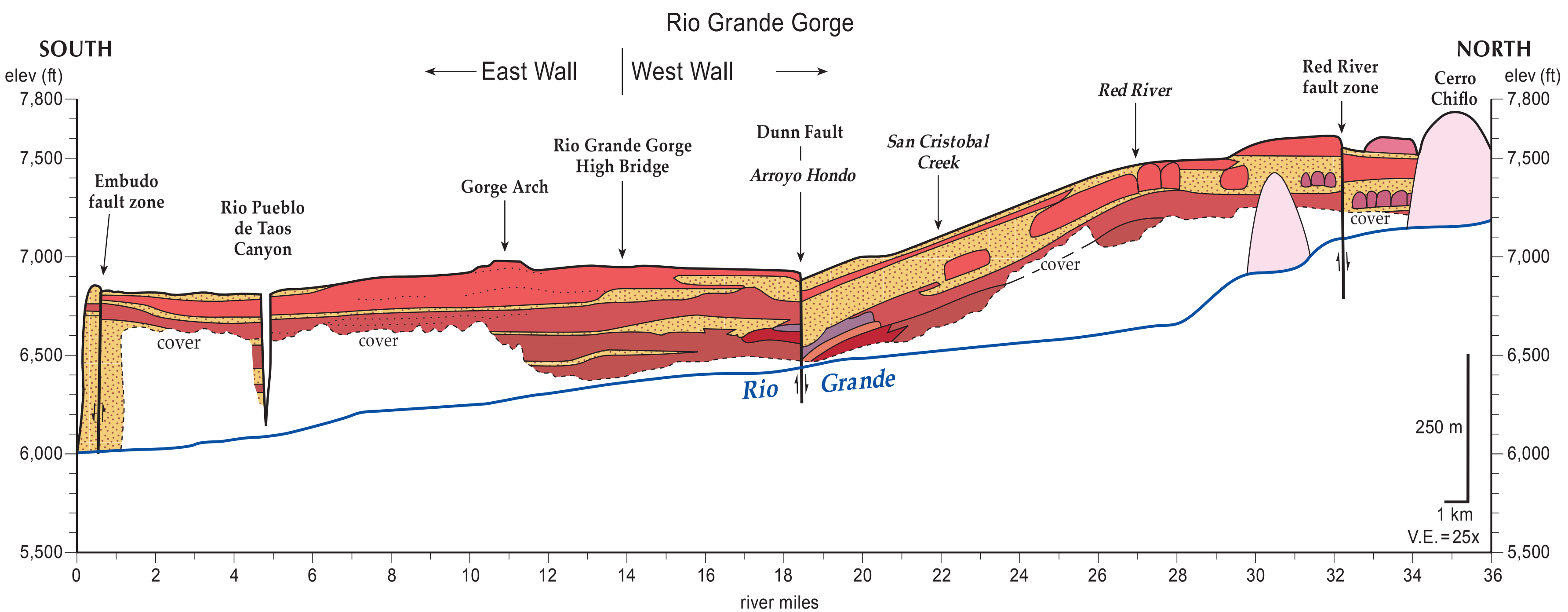

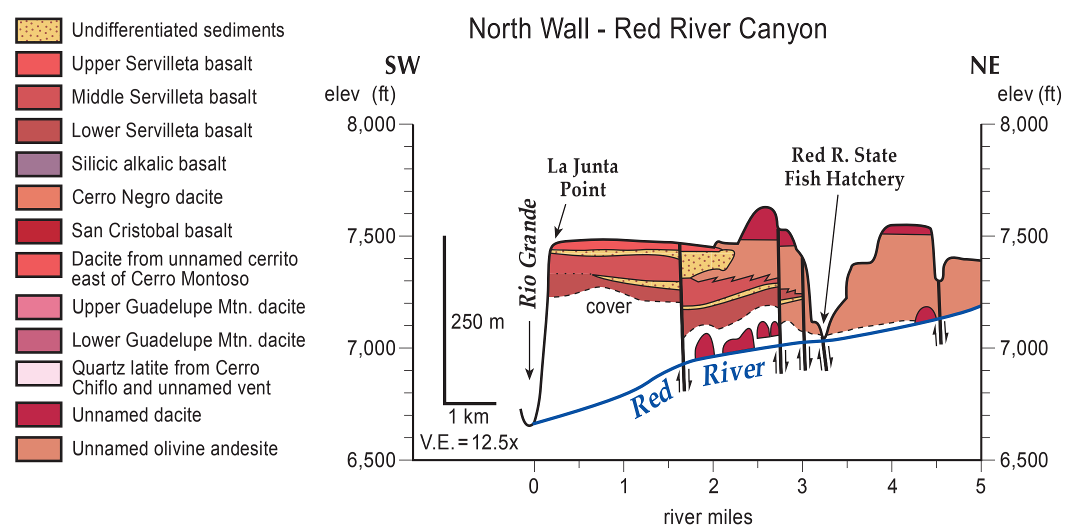

PLATE 10. Composite longitudinal profiles and cross sections of the volcanic stratigraphy exposed in the Rio Grande and Red River gorges. The data were compiled from scanned plates from the M.S. theses of Peterson (1981) and Leininger (1982). See roadlog references for complete citations.

PLATE 11: GEOLOGIC MAP OF THE VELARDE GRABEN – NORTHERN ESPAÑOLA BASIN

DANIEL J. KONING

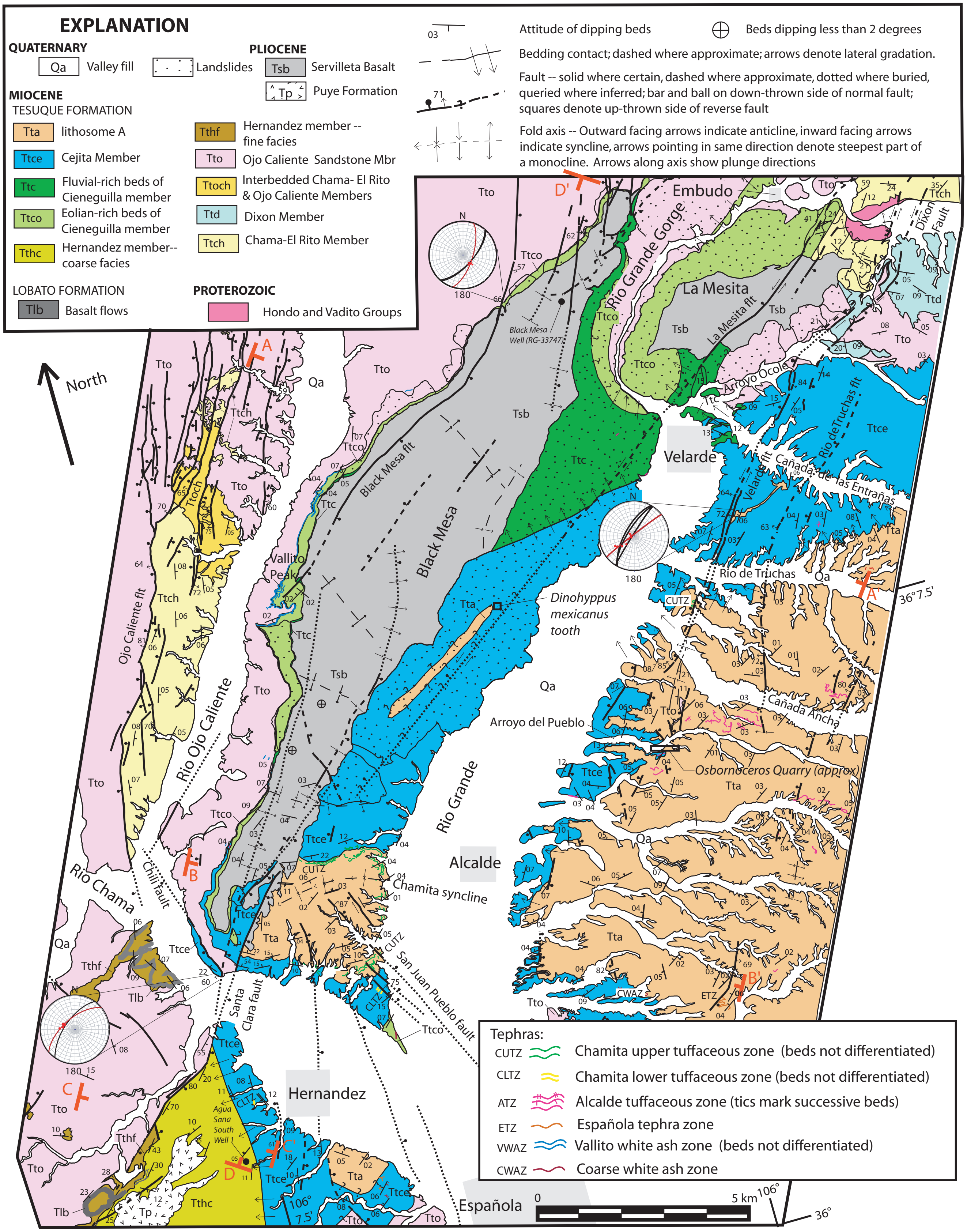

PLATE 11. Geologic map of the Velarde graben, northern Española Basin. Map compiled from Koning (2004), Koning and Aby (2003), Koning (2003), Koning and Manley (2003), with southwest part modified from Dethier and Manley (1985). Neogene terrace deposits are not shown. Stereonets of fault slickenside data are in Wulf equal-area projections. Black lines = measured fault planes. Red lines = best fit to data. Red, T-shaped lines show ends of cross sections discussed in Koning et al. (2004, this volume).

Taos Area Stratigraphy and Correlations for Proterozoic and Paleozoic

P.W. Bauer, K.E. Karlstrom, B.S. Kues, J.P. Dawson, M.T. Heizler, M.L. Williams, A.S. Read, D. Ulmer-Scholle

Era	Period	Picuris, Tusas & N. Rincon Mtns	S. Taos & Cimarron Ranges	N. Taos Range	Tectonic event
Mesozoic		None exposed			
Paleozoic	Per-mian	Sangre de Cristo Formation			Ancestral Rocky Mtn Orogeny
Paleozoic	Penn-sylvanian	Alamitos Formation			Ancestral Rocky Mtn Orogeny
Paleozoic	Penn-sylvanian	Flechado Formation			Ancestral Rocky Mtn Orogeny
Paleozoic	Mississippian	Arroyo Peñasco Group	Tererro Formation	Cowles Member Mañuelitas Member Turquillo Member Macho Member	Ancestral Rocky Mtn Orogeny
Paleozoic	Mississippian	Arroyo Peñasco Group	Espiritu Santo Formation	Carbonate member Del Padre Sandstone Member	Ancestral Rocky Mtn Orogeny
		The Great Unconformity			
Proterozoic	Neoprot-erozoic	Diabase dikes?	Diabase dikes?	Diabase dikes? / *1.0-0.96 Ga Ar-Ar muscovite (cooling through ~350C)*	Grenville Orogeny
Proterozoic	Mesoproterozoic	*1.35-1.27 Ga Ar-Ar muscovite (cooling through ~350C)* *1.5-1.3 Ga Ar-Ar hornblende (cooling through ~500C)*	*1.35 -1.19 Ga Ar-Ar muscovite (cooling through ~350C)* *1.40- 1.31 Ga Ar-Ar hornblendes (cooling through ~500C)*	*1.3-1.29 Ga Ar-Ar hornblendes (cooling through ~500C before 1.3 Ga)* *1.38 Ga U-Pb titanite (cooling through ~600-500C)* *1.42 Ga U-Pb metamorphic zircon growth*	Intracratonic Tectonism
Proterozoic	Mesoproterozoic	1.44 Ga Penasco quartz monzonite, 1.4 Ga Petaca pegmatites / *1.48-1.32 Ga U-Pb metamorphic monazite growth*	*1.43 Ga U-Pb metamorphic monazite growth*	1.42 Ga Pegmatite of Jaroso Canyon	Intracratonic Tectonism
Proterozoic	Mesoproterozoic	1.63-1.48 Ga regional stabilization of crust and tectonic lull. Rocks at approximately 10 km depth by 1.48 Ga.			Intracratonic Tectonism
Proterozoic	Paleoproterozoic	1.67 Ga Rana quartz monzonite, 1.68 Ga Puntiagudo granite, 1.68 Ga Guadalupita pluton	*1.68 Ga Ar-Ar hornblende from Quartz diorite of Cimarron River (cooling through ~500C)*	1.64 Ga Quartz monz. of Costilla Ck, 1.68 Ga Granodiorite of Jaracito Cn	Mazatzal Orogeny
Proterozoic	Paleoproterozoic	Hondo Group (Piedra Lumbre, Pilar, Rinconada, and Ortega Fms)	Hondo Group? (quartzite and pelitic schist)	Hondo Group? (quartzite and pelitic schist)	Mazatzal Orogeny
Proterozoic	Paleoproterozoic	Vadito Group (1.70 Ga Burned Mtn Fm, Glenwoody Fm, Marqueñas Fm, Big Rock Fm, schist, amphibolite) / 1.69 Ga Tres Piedras granite, 1.69 Ga Tusas granite, 1.7 Ga (Rb-Sr) Rio Brazos trondhjemite	Vadito Group? (layered gneiss; mafic, felsic, and pelitic gneiss, amphibolite) / 1.70 Ga Granite of Eagle Nest, 1.7 Ga Quartz monzonite of Old Mike Peak	Vadito Group? (layered gneiss; mafic, felsic, and pelitic gneiss, amphibolite)	Yavapai Orogeny .... Mazatzal Orogeny
Proterozoic	Paleoproterozoic		1.73 Ga Quartz monzonite of Columbine Creek	1.73 Ga Quartz monzonite of Columbine Creek	Yavapai Orogeny
Proterozoic	Paleoproterozoic		1.74 Ga Gold Hill metagabbro		Yavapai Orogeny
Proterozoic	Paleoproterozoic	1.75 Ga Maquinita granodiorite	1.75 Ga Tonalite of Red River		Yavapai Orogeny
Proterozoic	Paleoproterozoic	Moppin Complex (>1.76 Ga mafic-dominated schist & gneiss)	Gold Hill Complex (1.765 Ga mafic to felsic gneiss)		Yavapai Orogeny

All Proterozoic ages are U-Pb zircon unless otherwise noted. Data are from Armstrong & Mamet (1990), Grambling & Dallmeyer (1993), Karlstrom et al. (1997), Karlstrom et al. (2004), Lanzirotti & Hanson (1997), Lipman and Read (1989), Miller et al. (1963), Pedrick (1995), Read et al. (1999), Shaw et al. (in press), Ulmer & Laury (1984).